

Hamiltonian model of electromechanical actuator in natural reference frame.

Part I: Topology-based approximation algorithm

WOJCIECH BURLIKOWSKI

Department of Mechatronics, Faculty of Electrical Engineering

*Silesian University of Technology
Akademicka 10a, 44-100 Gliwice, Poland*

e-mail: wojciech.burlikowski@polsl.pl

(Received: 11.03.2011, revised: 26.05.2011)

Abstract: In the paper a novel mathematical model of electromechanical actuator is presented. It is based on application of Hamiltonian equations in the description of electromechanical energy conversion. It results in employment of flux linkages as state variables in the state space equations. For simplicity only a 3-phase wye connected stator winding without a neutral wire is considered in detail. The procedure can be generalised to any number of phases. Topology-based approach is used in the model implementation. Procedures for evaluation of all quantities (currents, energy/coenergy, electromagnetic torque) present in model equations are described. Eddy currents and hysteresis phenomenon are neglected in formulation of the model to enable application of state-space description.

Key words: Hamiltonian equations, simplex, simplicial complex, simplicial approximation, affine transformation

1. Introduction

In the paper a novel mathematical model of electromechanical actuator is presented. It is based on application of Hamiltonian equations in description of electromechanical energy conversion which results in employment of flux linkages as state variables in the state-space equations [37, 39]. The most important problem arising in this approach is evaluation of currents as function of flux linkages in multivariable space [7, 8, 39]. The proposed solution is based on the triangulation of databases (obtained using FEM [7, 8] or a measurement [26, 42]) and application of local linear (affine) homeomorphism between the spaces of variables [19] (space of currents and space of flux linkages). In algebraic topology this approach is defined as simplicial approximation [2, 16, 40, 44]. Similar approach is used in description of non-linear circuits and networks [9, 10, 23, 41].

2. Topology-based algorithm for approximation of current-flux linkage characteristics

2.1. Hamiltonian state-space equations

In matrix form the Hamiltonian state-space equations of electromechanical actuator can be written separately for electric and mechanical variables [39]:

$$\begin{aligned} \frac{d\Psi}{dt} &= \mathbf{u} - \mathbf{R} \mathbf{i}(\varphi, \Psi), \\ \frac{dK}{dt} &= T_e - T_m, \\ \frac{d\varphi}{dt} &= \frac{K}{J} \\ T_e &= -\frac{\partial E_{mag}(\varphi, \Psi)}{\partial \varphi} = \frac{\partial E_{cm}(\varphi, \mathbf{i})}{\partial \varphi}, \end{aligned} \quad (1)$$

where $\mathbf{i}(\varphi, \Psi)$ is the function that defines generalised currents in terms of rotor angular position φ and generalised flux linkages Ψ ; \mathbf{u} – generalised external voltages; \mathbf{R} – resistance matrix; T_e – electromagnetic torque; T_m – mechanical load torque; K – angular momentum; J – moment of inertia; E_{mag} – magnetic field energy; E_{cm} – magnetic field coenergy [P. II]. Energy and coenergy of magnetic field in actuator are defined by expressions:

$$E_{mag}(\varphi, \Psi) = \int_0^{\Psi} \mathbf{i} \cdot d\Psi = \int_0^{\Psi} \mathbf{i}^T d\Psi, \quad (2)$$

$$E_{cm}(\varphi, \mathbf{i}) = \int_0^{\mathbf{i}} \Psi \cdot d\mathbf{i} \quad (3)$$

and related by relationship [22, 37]:

$$E_{mag}(\varphi, \Psi) + E_{cm}(\varphi, \mathbf{i}) = \Psi^T \mathbf{i}. \quad (4)$$

In above formulas two forms of vector dot product representation used in this paper, vector and matrix, are shown.

The mathematical model of electromechanical actuator described by equation set (1) will be called **Hamiltonian Model of Electromechanical Actuator (HMEA)**. This abbreviation, which mimics commonly used convention in description of electromechanical actuators (SynRM, SRM, MCSRM, PMSM, BLDC, DTC etc.), will be used throughout the paper to distinguish the model among the other mathematical models of actuators.

2.2. General description

Evaluation of multivariable function $\mathbf{i}(\varphi, \Psi)$ in equation (1) is the most important issue in numerical implementation of HMEA [7, 37, 39].

In previous papers it was achieved with application of uniform databases and their interpolation. It employed „griddata3” numerical procedure [27]. The main drawback of this method was creation of large number of NaN (Not-a-Number) entries in the databases [7, 8].

In this paper a different methodology is proposed. It employs newly-introduced TriRep/DelaunayTri classes in Matlab'2009 [27]. These algorithms enable application of topology-based evaluation methodology using local piece-wise linear (affine) homeomorphism between current and flux linkage spaces [19]. In algebraic topology such transformation is defined as simplicial approximation [2, 16, 40, 44].

Numerical data for the primary databases used in description (Tab. 1) were obtained using the finite element analysis of a reluctance cageless synchronous motor [4, 8]. The structure of the databases is related with the specific evaluation methodology. In order to define the databases the following sets are used:

- the position set $\Theta = \{\varphi_1, \dots, \varphi_k, \dots, \varphi_K\}$ composed of K points where $\varphi_1 = 0$ [rad], $\varphi_K = \varphi_1 + 2\pi/p$ to account for symmetry, p – number of pole-pairs. Their choice depends on assumed resolution of the model (e.g. whether the model has to take account of only the fundamental space or also of the slotting effects etc. [24, 39]),
- for each angle $\varphi_k \in \Theta$ a current set I^k composed of $P(k)$ points is defined $I^k = \{i_1, \dots, i_p, \dots, i_{P(k)}\}$ where $i_p \in E^N$ (Tab. 1). The set I^k belongs to current subspace $RI^k \subset E^N$. Choice of I^k depends on the level of saturation and assumed maximum current of the device.

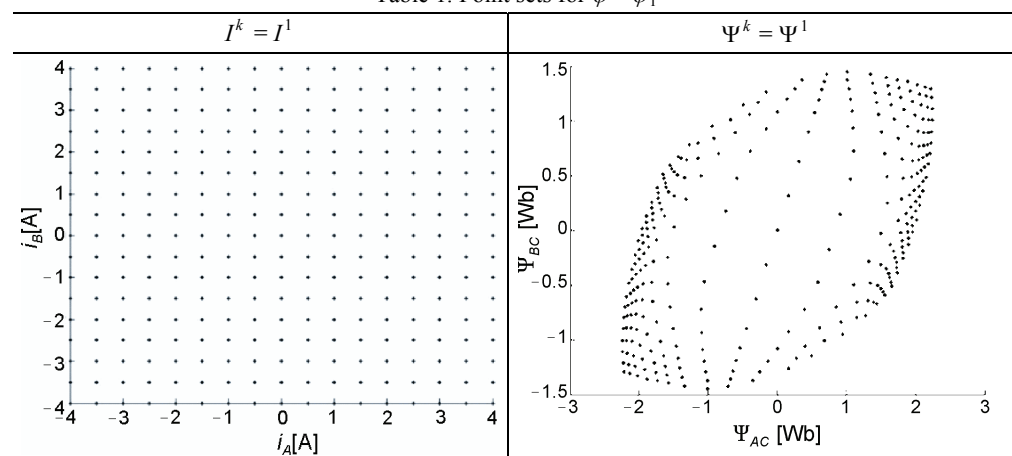
Dimension N of Euclidian space E^N is equal to the number of generalised (independent) variables which is $N=2$ in the presented example.

2.3. Methodology for $\varphi = \text{const}$

Applying FE calculation for arbitrary angle $\varphi_k \in \Theta$ one obtains two sets:

- the set of flux linkage points $\Psi^k = \{\Psi_1, \dots, \Psi_p, \dots, \Psi_{P(k)}\}, \Psi_p \in E^N$, (Tab. 1),
- the electromagnetic torque set $T_e(k) = \{T_{e,1}, \dots, T_{e,p}, \dots, T_{e,P(k)}\}$.

Table 1. Point sets for $\varphi = \varphi_1$



The Ψ^k set belongs to flux linkage subspace $\mathbf{R}\Psi^k \subset \mathbf{E}^N$ while torque set $T_e(k)$ consists of scalars $T_e(k) \subset \mathbf{E}^1$.

Values in $T_e(k)$ sets will be only used for comparison because an independent, autonomous algorithm for evaluation of electromagnetic torque will be developed in section (2.6).

As eddy currents and hysteresis phenomenon are neglected in the model, thus the function relationship f^k between the above mentioned subspaces $f^k : \mathbf{RI}^k \xrightarrow{\text{on}} \mathbf{R}\Psi^k$ is a homeomorphism [40, 44].

For such a function a local linear approximation f_A^k can be defined which has the following properties [2, 19, 40]:

- its domain is \mathbf{RI}^k defined with the help of approximation triplet $A^k = (I^k, \Psi^k, \mathbf{IK}^k)$ for which triangulation T^k (Tab. 3) defines a polyhedron $|T^k(I^k, \mathbf{IK}^k)| = \mathbf{RI}^k$ (Tab. 4). Abstract current simplicial complex \mathbf{IK}^k [2] defines combinatorial structure of triangulation T^k resulting from application of Delaunay's triangulation to the I^k set [12]. Obtained triangulation (Tab. 3) can be also defined as geometrical simplicial complex which consists of N -simplexes (0-simplex – vertex; 1-simplex – edge; 2-simplex – triangle; 3-simplex – tetrahedron) [2, 5, 40],
- $f_A^k(\mathbf{i}_p) = \Psi_p$,
- for an arbitrary j -th N -simplex $\Delta_{I^k,j} \in T^k(I^k, \mathbf{IK}^k)$ function $f_A^k(\mathbf{i})$ is affine on $\Delta_{I^k,j}$ and can be defined with the following formula [19]:

$$\Psi = f_A^k|_{\Delta_{I^k,j}}(\mathbf{i}) = \mathbf{C}^{k,j} (\mathbf{D}^{k,j})^{-1} \begin{bmatrix} \mathbf{i} \\ 1 \end{bmatrix} = \mathbf{C}^{k,j} \boldsymbol{\alpha}_{\Delta_{I^k,j}}(\mathbf{i}) = \mathbf{C}^{k,j} \boldsymbol{\alpha}^{k,j}(\mathbf{i}), \quad (5)$$

where:

$$\mathbf{C}^{k,j} = [\Psi_{j_1} \quad \Psi_{j_2} \quad \dots \quad \Psi_{j_{N+1}}], \quad \mathbf{D}^{k,j} = \begin{bmatrix} \mathbf{i}_{j_1} & \mathbf{i}_{j_2} & \dots & \mathbf{i}_{j_{N+1}} \\ 1 & 1 & & 1 \end{bmatrix}.$$

Values of $\boldsymbol{\alpha}^{k,j}(\mathbf{i})$ are barycentric coordinates of an arbitrary point $\mathbf{i} \in \Delta_{I^k,j}$ [2, 5]. Position of an arbitrary point \mathbf{i} in N -simplex $\Delta_{I^k,j}$ and its image $\Psi = f_A(\mathbf{i})$ in N -simplex $\Delta_{\Psi^k,j}$ is described with the same barycentric coordinates $\boldsymbol{\alpha}^{k,j}$ (Fig. 1) which will be used in the model numerical implementation.

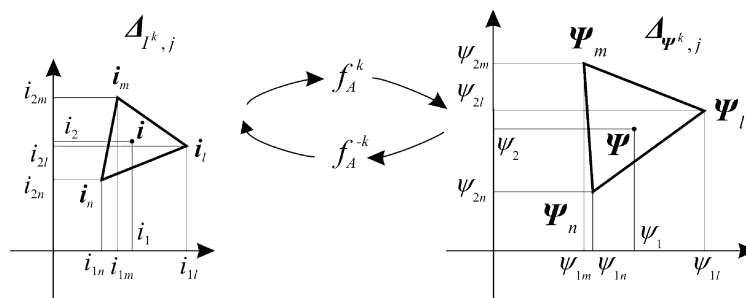
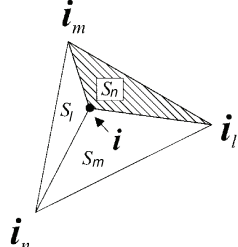


Fig. 1. Data for local invertible affine transformations on simplexes ($N=2$)

The reason for this important property is that affine transformations preserve barycentric coordinates [2, 5]. In case of $N=2$ which is analysed in the paper their geometric interpretation and basic properties are shown in Table 2.

Table 2. Properties of barycentric coordinates

	$\alpha^{k,j}(\mathbf{i}) = [\alpha_n \quad \alpha_l \quad \alpha_m]^T = \left[\frac{S_n}{S} \quad \frac{S_l}{S} \quad \frac{S_m}{S} \right]^T = \boldsymbol{\alpha}^{k,j}$ $\sum_{i=n, m, l} \alpha_i = 1; \quad \sum_{i=n, m, l} S_i = S; \quad \alpha_i \geq 0$ e.g. $\alpha^{k,j}(\mathbf{i} = \mathbf{i}_n) = [1 \quad 0 \quad 0]^T$ as $S_n(\mathbf{i} = \mathbf{i}_n) = S$, where S is the surface of the $\Delta_{I^k, j}$ simplex.
---	--

Equation (5) for $N=2$ presented in Figure 1 for an arbitrary j -th simplexes has a form:

$$\Psi = \begin{bmatrix} \psi_1 \\ \psi_2 \end{bmatrix} = \underbrace{\begin{bmatrix} \psi_{1n} & \psi_{1m} & \psi_{1l} \\ \psi_{2n} & \psi_{2m} & \psi_{2l} \end{bmatrix}}_{\mathbf{C}^{k,j}} \underbrace{\begin{bmatrix} i_{1n} & i_{1m} & i_{1l} \\ i_{2n} & i_{2m} & i_{2l} \\ 1 & 1 & 1 \end{bmatrix}}_{\mathbf{D}^{k,j}}^{-1} \underbrace{\begin{bmatrix} i_1 \\ i_2 \\ 1 \end{bmatrix}}_{\boldsymbol{\alpha}^{k,j}}. \quad (6)$$

For a homeomorphism f^k there exists an inverse function $f^{-k} : \mathbf{R}\Psi^k \xrightarrow{\text{on}} \mathbf{R}\mathbf{I}^k$. It enables a definition of its local linear approximation f_A^{-k} which has the following properties:

- its domain is $\mathbf{R}\Psi^k$ defined with the help of approximation triplet $A^{-k} = (\Psi^k, I^k, \mathbf{IK}^k)$ for which triangulation T^{-k} (Tab. 3) defines a polyhedron $|T^{-k}(\Psi^k, \mathbf{IK}^k)| = \mathbf{R}\Psi^k$ (Tab. 4) [16],
- $f_A^{-k}(\Psi_p) = \mathbf{i}_p$,

for an arbitrary j -th N -simplex $\Delta_{\Psi^k, j} \in T^{-k}(\Psi^k, \mathbf{IK}^k)$ function $f_A^{-k}(\mathbf{i})$ is affine on $\Delta_{\Psi^k, j}$ and can be defined with the following formulas

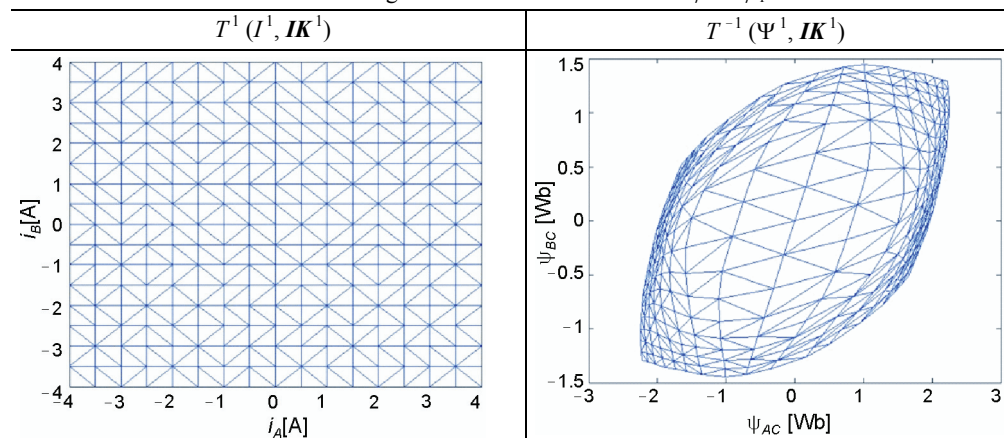
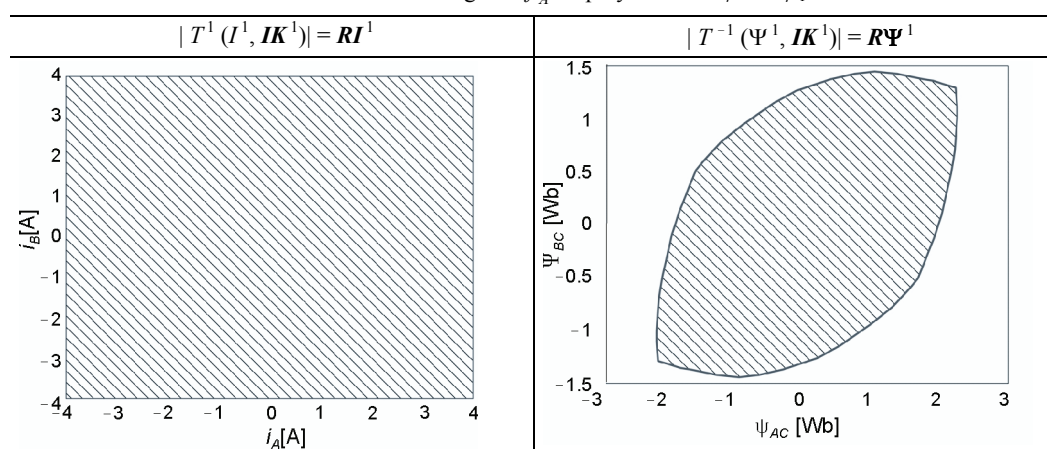
$$\mathbf{i} = f_A^{-k} \Big|_{\Delta_{\Psi^k, j}} (\Psi) = \begin{bmatrix} \mathbf{i}_{j_1} & \mathbf{i}_{j_2} & \dots & \mathbf{i}_{j_{N+1}} \end{bmatrix} \begin{bmatrix} \Psi_{j_1} & \Psi_{j_2} & \dots & \Psi_{j_{N+1}} \\ 1 & 1 & \dots & 1 \end{bmatrix}^{-1} \begin{bmatrix} \Psi \\ 1 \end{bmatrix}, \quad (7)$$

$$\mathbf{i} = \begin{bmatrix} \mathbf{i}_{j_1} & \mathbf{i}_{j_2} & \dots & \mathbf{i}_{j_{N+1}} \end{bmatrix} \boldsymbol{\alpha}_{\Delta_{\Psi^k, j}}(\Psi) = \begin{bmatrix} \mathbf{i}_{j_1} & \mathbf{i}_{j_2} & \dots & \mathbf{i}_{j_{N+1}} \end{bmatrix} \boldsymbol{\alpha}^{k,j}(\Psi). \quad (8)$$

Equation (7) for $N=2$ presented in Figure 1 for arbitrary j -th simplexes has a form:

$$\mathbf{i} = \begin{bmatrix} i_1 \\ i_2 \end{bmatrix} = \begin{bmatrix} i_{1n} & i_{1m} & i_{1l} \\ i_{2n} & i_{2m} & i_{2l} \end{bmatrix} \overbrace{\begin{bmatrix} \psi_{1n} & \psi_{1m} & \psi_{1l} \\ \psi_{2n} & \psi_{2m} & \psi_{2l} \\ 1 & 1 & 1 \end{bmatrix}}^{\alpha^{k,j}} \begin{bmatrix} \psi_1 \\ \psi_2 \\ 1 \end{bmatrix}. \quad (9)$$

A view of triangulations is shown in the Table 3. A view of polyhedra defined using these triangulations and representing domain and range of f^k for $\varphi = \varphi_1$ is shown in the Table 4. Exemplary data are shown in Tables 5 and 6.

Table 3. Triangulations used in the model for $\varphi = \varphi_1$ Table 4. Domain and range of f_A^1 as polyhedra for $\varphi = \varphi_1$ 

For polyhedra $\mathbf{R}I^k, \mathbf{R}\Psi^k$ (Tab. 4) which are convex hulls of appropriate point sets I^k, Ψ^k (Tab. 1) the simplicial approximation theorem applies. Its version for the above described structures can be defined as ([2] – page 381, theorem 7.2.8):

"For a continuous map $f^k : \mathbf{RI}^k \xrightarrow{\text{on}} \mathbf{R}\Psi^k$ and triangulations of its polyhedra $T^k(I^k, \mathbf{IK}^k)$, $T^{-k}(\Psi^k, \mathbf{IK}^k)$ for an arbitrary real number $\varepsilon > 0$ there exist barycentric subdivisions T_b^k of T^k , T_b^{-k} of T^{-k} such that its simplicial approximation $g: T_b^1 \xrightarrow{\text{on}} T_b^{-1}$ allows an approximating function f_A^k to meet a condition $\rho(f^k(\mathbf{i}), f_A^k(\mathbf{i})) < \varepsilon$ for each $\mathbf{i} \in \mathbf{RI}^k$ " where ρ is an Euclidian norm.

There are various versions of the theorem using different methods of proof ([16] – page 119, theorem 2.5.11; [40] – subchapter 3.4). Algorithm described in the paper is an application of that theorem. The theorem also defines the way to accuracy improvement by barycentric subdivision of existing triangulation [2]. Barycentric subdivision algorithm is very similar to mesh refinement in FEM [29].

Table 5. Flux linkages on triangulations

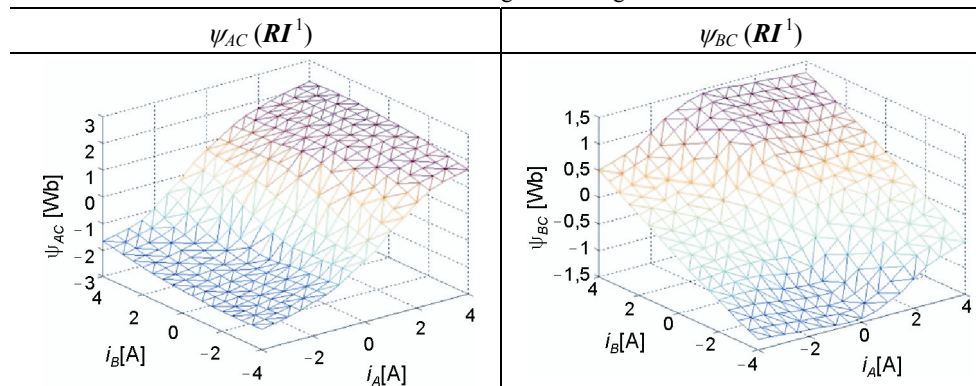
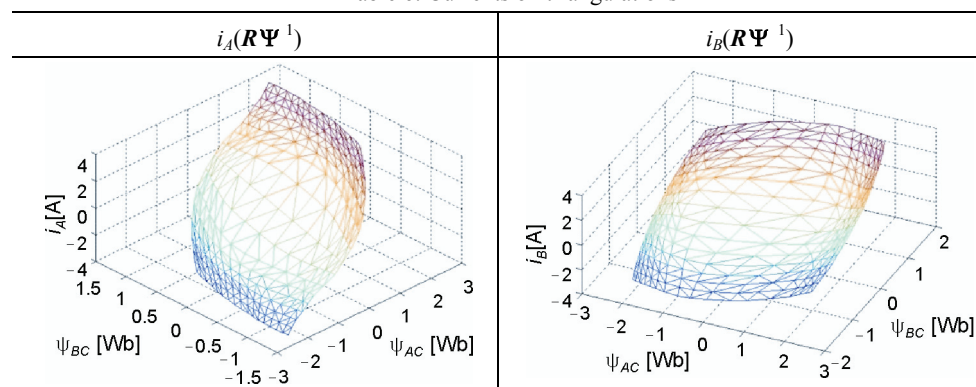


Table 6. Currents on triangulations



2.4. Evaluation of energy and coenergy for $\varphi = \text{const}$

Properties of affine transformation on simplexes (e.g. due to their convexity [2]) enable simple evaluation of line integrals which are necessary for calculation of energy and coenergy (Fig. 2). Using equations (2)(3) their increments along edges of simplexes can be obtained according to formulas:

$$\Delta E_{cm}^{m,l} = \int_{\mathbf{i}_m}^{\mathbf{i}_l} \boldsymbol{\Psi} \cdot d\mathbf{i}, \quad (10)$$

$$\Delta E_{mag}^{m,l} = \int_{\boldsymbol{\Psi}_m}^{\boldsymbol{\Psi}_l} \mathbf{i} \cdot d\boldsymbol{\Psi}, \quad (11)$$

for arbitrary vertices m, l (Fig. 1).

Line segments inside corresponding simplexes with an arbitrary vertex n as an end point (Fig. 2) can be defined as:

$$\mathbf{i}' \in [\mathbf{i}_n, \mathbf{i}] \Rightarrow \mathbf{i}' = \mathbf{i}_n + \gamma(\mathbf{i} - \mathbf{i}_n), \gamma \in [0, 1], \quad (12)$$

$$\boldsymbol{\Psi}' \in [\boldsymbol{\Psi}_n, \boldsymbol{\Psi}] \Rightarrow \boldsymbol{\Psi}' = \boldsymbol{\Psi}_n + \gamma(\boldsymbol{\Psi} - \boldsymbol{\Psi}_n), \gamma \in [0, 1]. \quad (13)$$

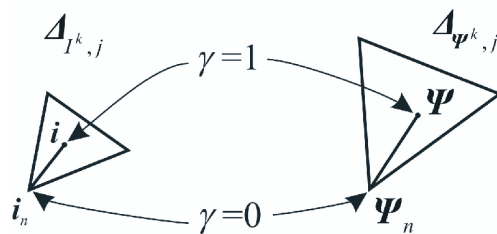


Fig. 2. Line segments, integration paths and parameters

In both cases the parameter γ is the same as line segments are mutual images of one another in the affine transformations f_A^k / f_A^{-k} [2]. The coenergy increment is:

$$\Delta E_{cm}^{m,l} = \int_{\mathbf{i}_m}^{\mathbf{i}_l} \boldsymbol{\Psi}' \cdot d\mathbf{i}' = \int_0^1 \boldsymbol{\Psi}' \cdot \frac{d\mathbf{i}'}{d\gamma} d\gamma = \int_0^1 (\boldsymbol{\Psi}_m + \gamma(\boldsymbol{\Psi}_l - \boldsymbol{\Psi}_m)) \cdot (\mathbf{i}_l - \mathbf{i}_m) d\gamma. \quad (14)$$

Integration gives the following result:

$$\Delta E_{cm}^{m,l} = \frac{1}{2} (\boldsymbol{\Psi}_l + \boldsymbol{\Psi}_m) \cdot (\mathbf{i}_l - \mathbf{i}_m). \quad (15)$$

Similar evaluation for energy leads to the result:

$$\Delta E_{mag}^{m,l} = \frac{1}{2} (\mathbf{i}_l + \mathbf{i}_m) \cdot (\boldsymbol{\Psi}_l - \boldsymbol{\Psi}_m). \quad (16)$$

Using the above results one obtains values of energy/coenergy in all vertices of the triangulation in the form of two sets $E_{cm}(k) = \{E_{cm,1}, \dots, E_{cm,p}, \dots, E_{cm,P(k)}\}$ and $E_{mag}(k) = \{E_{mag,1}, \dots, E_{mag,p}, \dots, E_{mag,P(k)}\}$ (Tab. 7). In the evaluation the reference vertex is the one with

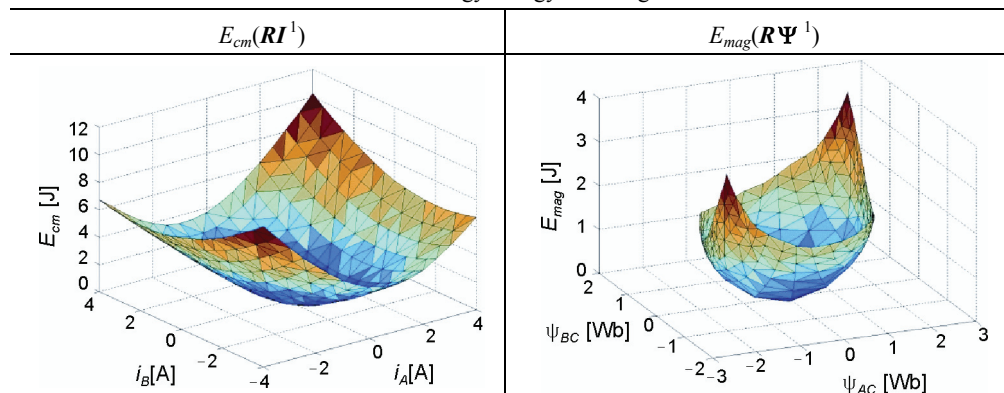
$E_{cm}(\varphi, \mathbf{i} = \mathbf{0}) = 0$, $E_{mag}(\varphi, \Psi = \mathbf{0}) = 0$ and the following ones are evaluated in series using the tree of the graph of triangulation [18].

Because there exists a relationship between E_{cm}/E_{mag} in the model, only coenergy is calculated and energy is obtained from equation (4). The reason is accuracy of data in sets I^k as they are inputs in FEM while data in Ψ^k are outputs of FEM calculations and thus are more error dependant [29]. Therefore, in an arbitrary point $\mathbf{i} \in \Delta_{I^k,j} \subset \mathbf{RI}^k$ only coenergy is calculated (Fig. 2).

$$E_{cm}|_{\Delta_{I^k,j}}(\varphi_k, \mathbf{i}) = E_{cm}(\varphi_k, \mathbf{i}_n) + \frac{1}{2}(\Psi + \Psi_n) \cdot (\mathbf{i} - \mathbf{i}_n). \quad (17)$$

This formula is equivalent to application of trapezoidal integration method which is exact for linear interpolation used in the model [2].

Table 7. Coenergy/energy on triangulations



2.5. Choice of angular interpolation method

Methodology presented in the previous part of the paper enables the evaluation of flux linkages, currents and energy/coenergy at an arbitrary point of spaces $\mathbf{R}\Psi^k \subset \mathbf{E}^N$, $\mathbf{RI}^k \subset \mathbf{E}^N$ at any constant angular position $\varphi_k \in \Theta$. Those spaces are only hyperplanes in the system configuration space \mathbf{E}^{N+1} representing both mechanical coordinate φ and electrical variables \mathbf{i} or Ψ . Depending on the choice of electrical variable the space to be analysed is either current space $\mathbf{I}\Theta \subset \mathbf{E}^{N+1}$ or flux linkage space $\Psi\Theta \subset \mathbf{E}^{N+1}$ [7].

In order to find approximations f^A/f^{-A} (Fig. 3b) for functions $f: \mathbf{I}\Theta \xrightarrow{\text{on}} \Psi\Theta$ / $f^{-1}: \Psi\Theta \xrightarrow{\text{on}} \mathbf{I}\Theta$ necessary for implementation of HMEA slightly different method will be applied than was used for $\varphi = \text{const}$. Its aim is preservation of standard approach used in analysis of electromechanical actuators [25]. It is based on separate treatment of mechanical and electrical variables which results from structure of system differential equations (1) [37, 39]. Similar situation also occurs in field models of electric machines due to problems with evaluation of electromagnetic torque and movement representation [13, 29].

The main problem is related to electromagnetic torque evaluation present in (1) [1, 11, 13]. Depending on the choice of variable it is described either as [43]:

$$T_e = -\frac{\partial E_{mag}(\varphi, \Psi)}{\partial \varphi} = -\frac{\partial}{\partial \varphi} \left[\int_0^{\Psi} \mathbf{i} \cdot d\Psi \right] \Big|_{\Psi=\text{const}} = -\int_0^{\Psi} \left[\frac{\partial \mathbf{i}}{\partial \varphi} \Big|_{\Psi=\text{const}} \right] \cdot d\Psi, \quad (18)$$

or

$$T_e = \frac{\partial E_{cm}(\varphi, \mathbf{i})}{\partial \varphi} = \frac{\partial}{\partial \varphi} \left[\int_0^i \Psi \cdot d\mathbf{i} \right] \Big|_{i=\text{const}} = \int_0^i \left[\frac{\partial \Psi}{\partial \varphi} \Big|_{i=\text{const}} \right] \cdot d\mathbf{i}. \quad (19)$$

The main conclusion that can be drawn from above equations is that the interpolation used in the evaluation of flux linkage/current as functions of an angle must be the same as for co-energy/energy. Otherwise, there would be an inconsistency in the model differential equations as the electromechanical energy conversion and torque development are the same phenomena [39, 43].

There are various possibilities in the choice of angular interpolation:

- piecewise constant interpolation [24],
- local linear interpolation which will be described below (Sec. 2.6),
- local cubic splines which are used in simulational model [P. II] [18],
- global Fourier series/FFT – which is the most common choice in the analysis of rotating electromechanical actuators [38, 39, 43].

In the paper only the local linear interpolation in $\mathbf{I}\Theta / \Psi\Theta$ is described as the natural continuation of approach used in $\mathbf{R}\Psi^k \subset \mathbf{E}^N, \mathbf{RI}^k \subset \mathbf{E}^N$.

2.6. Evaluation of variables as function of an angle ($\varphi = \text{var}$)

Assuming that the state of the system at time instant t is described by Hamiltonian variables $[\varphi(t), K(t), \Psi^T(t)]$ then the following quantities must be evaluated in order to integrate the state space equations(1):

- current $\mathbf{i}(t)$ using known approximations $f_A^{-k}, f_A^{-(k+1)}$, at φ_k and φ_{k+1} where $\varphi \in < \varphi_k, \varphi_{k+1} >$,
- electromagnetic torque $T_e(t)$.

Algorithm of current $\mathbf{i}(t)$ evaluation can be divided into the following steps (Fig. 3):

- create projection (mapping) of $\Psi(t)$ on hyperplanes $\mathbf{R}\Psi^k \cap \mathbf{R}\Psi^{k+1}$,
- find two N -simplexes $\Delta_{\Psi^k, n}, \Delta_{\Psi^{k+1}, m}$, such that: $\Psi(t) \in \Delta_{\Psi^k, n} \subset \mathbf{R}\Psi^k, \Psi(t) \in \Delta_{\Psi^{k+1}, m} \subset \mathbf{R}\Psi^{k+1}$, using TriRep structure in Matlab [27] (Fig. 3a),
- evaluate barycentric coordinates $\alpha^{k, n}(\Psi(t)), \alpha^{k+1, m}(\Psi(t))$,
- evaluate currents

$$\mathbf{i}^{k, n} = f_A^{-k} \Big|_{\Delta_{\Psi^k, n}} (\Psi(t)), \quad \mathbf{i}^{k+1, m} = f_A^{-(k+1)} \Big|_{\Delta_{\Psi^{k+1}, m}} (\Psi(t))$$

using equation (7),

- evaluate unknown current using linear interpolation (Fig. 3b)

$$\mathbf{i}(t) = \mathbf{i}^{k,n} + (\mathbf{i}^{k+1,m} - \mathbf{i}^{k,n})\beta, \quad (20)$$

where:

$$\beta = \frac{\varphi - \varphi^k}{\varphi^{k+1} - \varphi^k}$$

as an image of a line segment in affine transformation is another line segment (Fig. 3b).

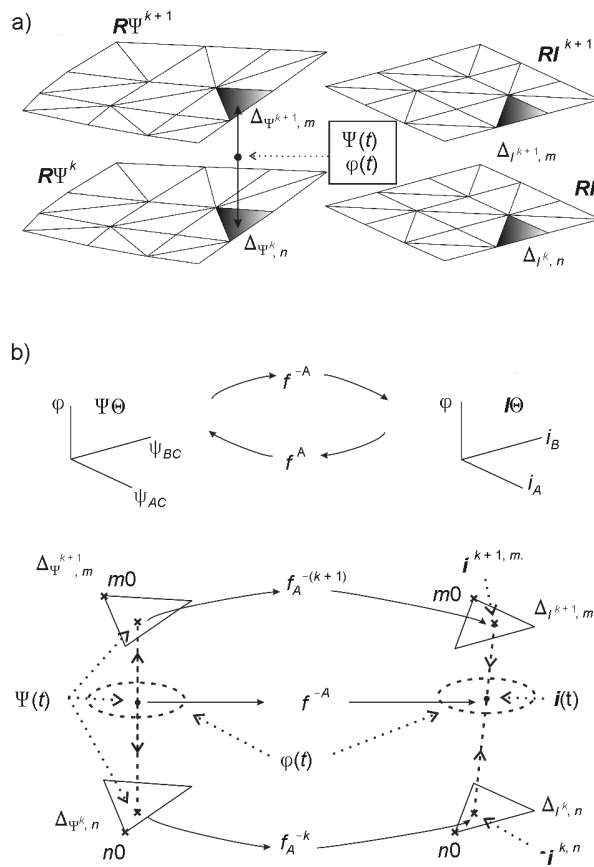


Fig. 3. Current evaluation a) choice of simplexes, b) interpolation

To evaluate torque T_e for angle $\varphi \in \langle \varphi_k, \varphi_{k+1} \rangle$ one must use the following integral:

$$\int_{\varphi_k}^{\varphi_{k+1}} T_e d\varphi \Big|_{\Psi=\text{const}} = - \int_{\varphi_k}^{\varphi_{k+1}} \frac{\partial E_{mag}(\varphi, \Psi(t))}{\partial \varphi} d\varphi = \dots \quad (21)$$

$$\dots = E_{mag}(\varphi_k, \Psi(t)) - E_{mag}(\varphi_{k+1}, \Psi(t)).$$

In case of linear current interpolation (20) the calculated torque T_e is equal to an average value T_e^{Avg} of the torque integral in equation (21) as for linear interpolation of energy its differential vs. angle is constant:

$$T_e(\varphi, \Psi) = T_e^{\text{Avg}}(\varphi \in \langle \varphi_k, \varphi_{k+1} \rangle, \Psi) = \frac{E_{\text{mag}}(\varphi_k, \Psi(t)) - E_{\text{mag}}(\varphi_{k+1}, \Psi(t))}{\varphi_{k+1} - \varphi_k}. \quad (22)$$

Using the quantities already obtained during current $\mathbf{i}(t)$ evaluation the torque is calculated as follows:

$$E_{\text{mag}}(\varphi_k, \Psi(t)) = E_{\text{mag}}(\varphi_k, \Psi_{n0}) + \frac{1}{2}(\mathbf{i}^{k,n} + \mathbf{i}_{n0}) \cdot (\Psi(t) - \Psi_{n0}), \quad (23)$$

$$E_{\text{mag}}(\varphi_{k+1}, \Psi(t)) = E_{\text{mag}}(\varphi_{k+1}, \Psi_{m0}) + \frac{1}{2}(\mathbf{i}^{k+1,m} + \mathbf{i}_{m0}) \cdot (\Psi(t) - \Psi_{m0}), \quad (24)$$

$$T_e(t) = \frac{E_{\text{mag}}(\varphi_k, \Psi(t)) - E_{\text{mag}}(\varphi_{k+1}, \Psi(t))}{\varphi_{k+1} - \varphi_k}, \quad (25)$$

where $n0$ is an arbitrary vertex of N -simplex $\Delta_{\Psi^k, n}$, $m0$ is an arbitrary vertex of N -simplex $\Delta_{\Psi^{k+1}, m}$, (Fig. 3).

A modification of this algorithm is necessary when $\varphi(t) = \varphi_k$. The algorithm must be performed twice for two pairs of hyperplanes:

- $\mathbf{RI}^{k-1}, \mathbf{RI}^k$ – which gives

$$T_e^{k-1,k}(t) = \frac{E_{\text{mag}}(\varphi_{k-1}, \Psi(t)) - E_{\text{mag}}(\varphi_k, \Psi(t))}{\varphi_k - \varphi_{k-1}},$$

- $\mathbf{R}\Psi^k, \mathbf{R}\Psi^{k+1}$ – which gives

$$T_e^{k,k+1}(t) = \frac{E_{\text{mag}}(\varphi_k, \Psi(t)) - E_{\text{mag}}(\varphi_{k+1}, \Psi(t))}{\varphi_{k+1} - \varphi_k}.$$

It gives the final value of the torque equal to their average as an analogy to method used in Fourier series method at a point of a step change:

$$T_e(\varphi(t) = \varphi_k, \Psi(t)) = \frac{1}{2}(T_e^{k-1,k}(t) + T_e^{k,k+1}(t)). \quad (26)$$

Those formulas can be easily implemented in the simulation model using user-defined function in Matlab/SIMULINK environment [27].

3. Conclusions

Main capabilities of proposed HMEA implementation are based on assumed topology of databases (local linear homeomorphism [19, 40]). Similar approach has been used in de-

scription of electronic nonlinear circuits and networks for decades [41]. To apply this approach for electromechanical actuators one must use proper current sets I^k , $k \in \{1, \dots, K\}$ (Tab. 1) to ensure that local behaviour of analysed variables can be treated as linear. The solution of this problem could be found in procedures used in Finite Element Analysis FEA [29].

References

- [1] Arkkio A., Hannukainen A., Niemenmaa A., *Power balance for verifying torque computation within time-discretized finite-element analysis*. XXI Symposium Electromagnetic Phenomena in Nonlinear Circuits EPNC', Germany, Dortmund and Essen, pp. 23-24 (2010).
- [2] Agoston M.K., *Computer graphics and geometric modeling – mathematics*. Springer (2005).
- [3] Boldea I., Nasar S.A., *Electric drives*. Taylor&Francis (2005).
- [4] Boldea I., *Reluctance synchronous machines & drives*. Oxford Univ. Press (1996).
- [5] Borsuk K., *Multidimensional analytical geometry*. PWN, Warsaw (1977) (in Polish).
- [6] Brown J.E., Kovacs K.P., Vas P., *A method of including the effects of main flux path saturation in generalised equations of A.C. machines*. IEEE Transactions on Power Apparatus and Systems, PAS-102(1): 96-103 (1983).
- [7] Burlikowski W., *Mathematical model of an electromechanical actuator using flux state variables applied to reluctance motor*. COMPEL 25(1): 169-180 (2006).
- [8] Burlikowski W., *Influence of saturation modelling method on results obtained using different implementations of reluctance motor simulational model*. XX Symposium Electromagnetic Phenomena in Nonlinear Circuits EPNC'2008, France, Lille, July, pp. 69-70 (2008).
- [9] Chua L.O., Desoer C.A., Kuh E.S., *Linear and nonlinear circuits*. McGraw-Hill (1987).
- [10] Chua L.O., McPherson J.D., *Explicit topological formulation of lagrangian and hamiltonian equations for nonlinear networks*. IEEE Transactions on Circuits and Systems CAS-21(2), March, pp. 277-286 (1974).
- [11] Coulomb J.I., *A methodology for determination of global electromechanical quantities from a finite element analysis and its application to the evaluation of magnetic forces, torques and stiffness*. IEEE Trans. Magn. 19, pp. 25 14-25 19, November (1983).
- [12] De Berg M., Van Kreveld M., Overmars M., Schwarzkopf O., *Computational geometry*, Springer (2000).
- [13] Demenko A., *Movement simulation in finite element analysis of electric machine dynamics*. IEEE Transactions on Magnetics 32(3): 1553-1556 (1996).
- [14] Demenko A., *Time-stepping FE analysis of electric motor drives with semiconductor converters*. IEEE Transactions on Magnetics 30(5): 3264-3267 (1994).
- [15] Demenko A., Hameyer K., *Field and field-circuit description of electrical machines*. Proc. of EPE-PEMC, pp. 2412-2419 (2008).
- [16] Engelking R., Sieklucki K., *Introduction to topology*. PWN (1986) (in Polish).
- [17] Fryze S., *Selected problems of theoretical basis of electrical engineering*. PWN, Warsaw-Wroclaw (1966) (in Polish).
- [18] Goodman J.E., O'Rourke J., et al. *Handbook of discrete and computational geometry*. CRC Press (1997).
- [19] Groff R.E., *Piecewise linear homeomorphisms for approximation of invertible maps*. Ph.D. Thesis, Univ. of Michigan (2003).
- [20] Hu, Y., Torrey, D.A., *Study of the mutually coupled switched reluctance machine using the finite element-circuit coupled method*. IEE Proceedings – Electric Power Applications 149(2): 81-86 (2002).
- [21] Jagieła M., Grabiec T., *Coupling electromagnetic (FE) models to multidomain simulator to analyse electrical driver and complex control systems*. AEE 59(3-4): 189-201 (2010).
- [22] Jeltsema D., Scherpen J.M.A., *Multidomain modeling of nonlinear networks and systems*. IEEE Control Systems Magazine, August, pp. 28-59 (2009).

- [23] Kang S.M., Chua L.O., *A global representation of multidimensional piecewise-linear functions with linear partitions*. IEEE Transactions on Circuits and Systems CAS-25(11): 938-940 (1978).
- [24] Kluszczyński K., Spalek D., *Step-by-step analysis of induction machines allowing for slotting*. Polish Society for Theoretical and Applied Electrical Engineering, Warsaw (2002).
- [25] Krause P., *Analysis of electric machinery*. McGraw-Hill (1986).
- [26] Ludwinek K., Siedlarz A., *Harmonic distortion analysis in armature currents of synchronous machine during co-operation with the power system*. Zeszyty Problemowe Maszyny Elektryczne 84: 217-223 (2009).
- [27] Matlab on-line Manual. R2010a, 2010.
- [28] Meeker D., *Finite element method magnetics*. User's Manual, Ver. 4.2 (2007).
- [29] Meunier G., et al., *The finite element method for electromagnetic modelling*. ISTE Ltd (2008).
- [30] Nehl T.W., Fouad F.A., Demerdash N.A., *Determination of saturated values of rotating machinery incremental and apparent inductances by an energy perturbation method*. IEEE Transactions on Power Apparatus and Systems PAS-101(11): 4441-4451 (1982).
- [31] Nowak, L., *Dynamic operation of an electromechanical actuator*. COMPEL18(4): 611-618 (1999).
- [32] Ozturk S.B., Toliyat H.A., *Sensorless direct torque and indirect flux control of brushless DC motor with non-sinusoidal back-EMF*. Proc. IEEE-IECON Annu. Meeting, Orlando, pp. 1373-1378 (2008).
- [33] Park R.H., *Two-reaction theory of synchronous machines – generalized method of analysis – Part I*. AIEE Trans. 48: 716-727 (1929).
- [34] Paszek W., *Dynamics of alternating current electric machines*, Helion, Gliwice (1998) (in Polish).
- [35] Puchała A., *Dynamics of machines and electromechanical systems*. PWN, Warsaw (1977) (in Polish).
- [36] Schlensok Ch., Henneberger G., *Simulation of a PMSM with SIMPLORER-FLUX2D-Coupling*. CD-ROM Proc. of XVth ICEM'2002, Brugge-Belgium, August (2002).
- [37] Schmitz N.L., Novotny D.W., *Introductory electromechanics*. The Ronald Press Company, New York (1965).
- [38] Sobczyk T.J., *Inductanceless model of salient-pole synchronous machines*. Proc. of SPEEDAM, pp. 620-625 (2008).
- [39] Sobczyk T.J., *Methodological aspects of mathematical modeling of induction machines*. WNT, Warsaw (2004) (in Polish).
- [40] Spanier E.H., *Algebraic topology*. McGraw-Hill Series in Higher Mathematics (1972).
- [41] Stern T.E., *Piecewise-linear network theory*. MIT, Research Laboratory of Electronics, Technical Report 315 (1956).
- [42] Stumberger G., Stumberger B., Dolinar D., *Identification of linear synchronous reluctance motor parameters*. IEEE Transactions On Industry Applications 40(5): 1317-1324 (2004).
- [43] Wach P., *Devices for electromechanical energy conversion*. Opole (1991) (in Polish).
- [44] Zomorodian A.J., *Topology for computing*. Cambridge Monographs on Applied and Computational Mathematics (2005).
- [45] Zunoubi M.R., Payne J., Roach W.P., *CUDA Implementation of TEz-FDTD solution of Maxwell's equations in dispersive media*. IEEE Antennas and Wireless Propagation Letters 9: 756-759 (2010).
[P. II] Part II of the paper.